

Treatment of Orthotopic U251 Human Glioblastoma Multiforme Tumors in NRG Mice by Convection-Enhanced Delivery of Gold Nanoparticles Labeled with the β -Particle-Emitting Radionuclide, ^{177}Lu

Constantine J. Georgiou, Zhongli Cai, Noor Alsaden, Hyungjun Cho, Minou Behboudi, Mitchell A. Winnik, James T. Rutka, and Raymond M. Reilly*



Cite This: <https://doi.org/10.1021/acs.molpharmaceut.2c00815>



Read Online

ACCESS |



Metrics & More

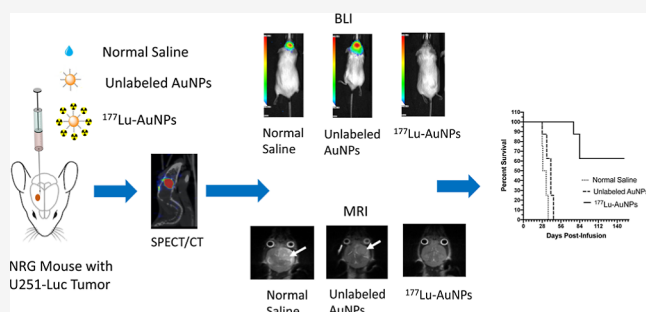


Article Recommendations



Supporting Information

ABSTRACT: In this study, we investigated convection-enhanced delivery (CED) of 23 ± 3 nm gold nanoparticles (AuNPs) labeled with the β -particle-emitting radionuclide ^{177}Lu (^{177}Lu -AuNPs) for treatment of orthotopic U251-Luc human glioblastoma multiforme (GBM) tumors in NRG mice. The cytotoxicity in vitro of ^{177}Lu -AuNPs (0.0–2.0 MBq, 4×10^{11} AuNPs) on U251-Luc cells was also studied by a clonogenic survival assay, and DNA double-strand breaks (DSBs) caused by β -particle emissions of ^{177}Lu were measured by confocal immunofluorescence microscopy for γH2AX . NRG mice with U251-Luc tumors in the right cerebral hemisphere of the brain were treated by CED of 1.1 ± 0.2 MBq of ^{177}Lu -AuNPs (4×10^{11} AuNPs). Control mice received unlabeled AuNPs or normal saline. Tumor retention of ^{177}Lu -AuNPs was assessed by single-photon emission computed tomography/computed tomography (SPECT/CT) imaging and biodistribution studies. Radiation doses were estimated for the tumor, brain, and other organs. The effectiveness for treating GBM tumors was determined by bioluminescence imaging (BLI) and T2-weighted magnetic resonance imaging (MRI) and by Kaplan–Meier median survival. Normal tissue toxicity was assessed by monitoring body weight and hematology and blood biochemistry analyses at 14 d post-treatment. ^{177}Lu -AuNPs (2.0 MBq, 4×10^{11} AuNPs) decreased the clonogenic survival of U251-Luc cells to 0.005 ± 0.002 and increased DNA DSBs by 14.3-fold compared to cells treated with unlabeled AuNPs or normal saline. A high proportion of ^{177}Lu -AuNPs was retained in the U251-Luc tumor in NRG mice up to 21 d with minimal re-distribution to the brain or other organs. The radiation dose in the tumor was high (599 Gy). The dose in the normal right cerebral hemisphere of the brain excluding the tumor was 93-fold lower (6.4 Gy), and 2000–3000-fold lower doses were calculated for the contralateral left cerebral hemisphere (0.3 Gy) or cerebellum (0.2 Gy). The doses in peripheral organs were <0.1 Gy. BLI revealed almost complete tumor growth arrest in mice treated with ^{177}Lu -AuNPs, while tumors grew rapidly in control mice. MRI at 28 d post-treatment and histological staining showed no visible tumor in mice treated with ^{177}Lu -AuNPs but large GBM tumors in control mice. All control mice reached a humane endpoint requiring sacrifice within 39 d (normal saline) or 45 d post-treatment (unlabeled AuNPs), while 5/8 mice treated with ^{177}Lu -AuNPs survived up to 150 d. No normal tissue toxicity was observed in mice treated with ^{177}Lu -AuNPs. We conclude that CED of ^{177}Lu -AuNPs was highly effective for treating U251-Luc human GBM tumors in the brain in NRG mice at amounts that were non-toxic to normal tissues. These ^{177}Lu -AuNPs administered by CED hold promise for treating patients with GBM to prevent recurrence and improve long-term outcome.



KEYWORDS: glioblastoma multiforme, gold nanoparticles, ^{177}Lu , β -particles, radiation treatment, convection-enhanced delivery

INTRODUCTION

Glioblastoma multiforme (GBM) is the most common and most lethal primary brain tumor.¹ Despite current standard-of-care treatment, the median survival of patients with GBM is poor (15–16 months), and the 5 year survival is only 5%.² GBM is treated by surgical excision followed by fractionated radiotherapy (60 Gy) and concurrent temozolomide chemotherapy (75 mg/m²/day for 6 weeks).³ Unfortunately, residual

Received: September 25, 2022

Revised: November 27, 2022

Accepted: November 29, 2022

tumor post-treatment leads to recurrence, causing death. Most recurrences are present within 2 cm of the surgical margins.⁴ Thus, strategies to eradicate residual tumor could reduce GBM recurrence and improve patient survival. However, a challenge is the blood–brain barrier (BBB) which limits the delivery of intravenously (i.v.) injected therapeutic agents to the brain.⁵ An exception is temozolomide which is able to penetrate the BBB.⁶ Various technologies are being explored to improve drug transport across the BBB.⁷ However, an approach which bypasses the BBB is convection-enhanced delivery (CED), a technique that creates a pressure gradient using an external pump to slowly infuse (0.1–10 $\mu\text{L}/\text{min}$) therapeutic agents into the brain via one or more catheters inserted into the tumor under image guidance.^{8,9} This approach has been investigated for delivery of chemotherapeutic drugs, toxins, liposomes, and viruses to tumors in pre-clinical mouse GBM models and in patients with GBM.⁸

Locoregional administration of radiotherapeutic agents emitting α -particles or β -particles holds promise for treatment of GBM.¹⁰ One approach previously studied clinically was infusion of radiolabeled monoclonal antibodies through a catheter inserted into the surgical cavity in patients with GBM.¹¹ Reardon et al. treated patients with GBM by infusion of anti-tenascin-C antibodies labeled with β -particle emitter, ¹³¹I.¹² Encouraging results were obtained with the median survival of patients diagnosed with GBM exceeding 21 months and >16 months in patients with recurrent GBM. 81C6 antibodies labeled with the α -particle emitter, ²¹¹At, provided a median survival of 12 months in patients with recurrent GBM.¹³ Another class of radiotherapeutic agents which have been studied preclinically for treatment of GBM via CED is radiolabeled nanoparticles (NPs).¹⁴ However, these studies have been limited to liposomes, lipid nanocapsules, or metallofullerenes. Phillips et al. treated nude rats with orthotopic U87 human GBM tumors by CED of ¹⁸⁶Re-labeled liposomes (0.9–4.6 MBq). ¹⁵¹⁸⁶Re ($t_{1/2} = 3.8$ d) emits moderate energy β -particles ($E\beta_{\text{max}} = 1.08$ MeV) that have a maximum range in tissues of 4.8 mm.¹⁶ Single-photon emission computed tomography (SPECT) imaging using ^{99m}Tc-labeled liposomes revealed confinement to the tumor in the brain following CED. ¹⁸⁶Re-liposomes strongly inhibited tumor growth assessed by bioluminescence imaging (BLI) or magnetic resonance imaging (MRI). The median survival increased >2.5 fold from 49 d for control rats to 126 d for rats receiving ¹⁸⁶Re-liposomes. There was no evidence of toxicity. ¹⁸⁶Re-liposomes were more effective for treating U251 human GBM tumors with >80% of rats surviving >130 d compared to <30 d for control rats. Vanpouille-Box et al. treated Fisher rats with 9L rat glioma tumors with lipid nanocapsules labeled with ¹⁸⁸Re in fractionated amounts (2.8 MBq). ¹⁷¹⁸⁸Re ($t_{1/2} = 16.9$ h) emits higher energy β -particles ($E\beta_{\text{max}} = 2.12$ MeV) that have a maximum range in tissues of 10.4 mm.¹⁶ An injection of 10 μL of ¹⁸⁸Re-nanocapsules at 1 $\mu\text{L}/\text{min}$ at 12 d after tumor implantation, followed by a second administration by CED of 60 μL at 0.5 $\mu\text{L}/\text{min}$ at 18 d, eradicated tumors in the brain and increased survival to >120 d in 5/6 treated rats compared to <30 d in control rats.¹⁷ In contrast, Huang et al. treated Fisher rats with F98 rat glioma tumors by intravenous (i.v.) injection of much higher amounts (333 MBq) of ¹⁸⁸Re-labeled liposomes.¹⁸ Only ~2% of the injected dose/g (% ID/g) accumulated in the tumor. Disappointingly, the median survival of treated rats was only marginally increased to 20 d

compared to 18 d for control rats, and body weight decreased, indicating toxicity.¹⁸ Comparison of the abovementioned two studies clearly demonstrated the superiority of locoregional delivery of radiolabeled NPs for treatment of GBM over systemic (i.v.) administration. Shultz et al. constructed metallofullerenes labeled with ¹⁷⁷Lu.¹⁹¹⁷⁷Lu ($t_{1/2} = 6.7$ d) emits moderate energy β -particles ($E\beta_{\text{max}} = 0.497$ MeV) with a maximum range in tissues of 1.8 mm.¹⁶ CED of ¹⁷⁷Lu-labeled metallofullerenes (0.25–1.35 MBq) into U87MG tumors in nude mice yielded a dose-dependent increase in survival with >80% of mice treated with 1.35 MBq surviving >100 d, while control mice survived <29 d. Tumors in the brain in treated mice were smaller than in control mice assessed by ex vivo histological staining.²⁰

One class of radiolabeled NPs that has not been studied for treatment of GBM via CED is gold NPs (AuNPs), despite their effectiveness for treatment of tumors outside the brain after local intratumoral (i.t.) injection with minimal toxicity.^{14,21} For example, our group treated athymic mice with subcutaneous MDA-MB-468 human breast cancer (BC) tumors by i.t. injection of AuNPs labeled with ¹⁷⁷Lu (4.5 MBq).²² Tumor growth was arrested in mice receiving ¹⁷⁷Lu-AuNPs, while untreated mice exhibited rapid and exponential tumor growth. No normal tissue toxicity was found, assessed by hematological and serum biochemical analysis and by monitoring body weight. The ¹⁷⁷Lu-AuNPs were confined to the i.t. injection site, providing high concentrations in the tumor (>300–400% ID/g) but very low uptake in normal tissues (<0.5% ID/g). The radiation absorbed dose in the tumor was 20–30 Gy, while normal organs received <1 Gy. Based on these encouraging results in a subcutaneous (s.c.) BC tumor xenograft model, we hypothesized in the current study that ¹⁷⁷Lu-AuNPs administered via CED would be effective for treating orthotopic U251-Luc human GBM xenografts in NOD-Rag1^{null}IL2rg^{null} (NRG) mice at amounts that are non-toxic. Our results demonstrate, for the first time, that CED of ¹⁷⁷Lu-AuNPs (1.1 \pm 0.2 MBq) strongly inhibited the growth of U251-Luc tumors in the brain of NRG mice, resulting in very small or undetectable tumors imaged by BLI and MRI, which significantly prolonged the median survival of treated mice compared to control mice by up to 3.8-fold, without normal tissue toxicity. These results hold promise for ¹⁷⁷Lu-AuNPs administered by CED for treatment of GBM in patients, potentially to eliminate residual disease, prevent recurrence, and improve patient outcome.

■ MATERIALS AND METHODS

Synthesis and Characterization of ¹⁷⁷Lu-AuNPs and Cytotoxicity In Vitro. AuNPs (23 \pm 3 nm) were synthesized by the Turkevich method.²³ AuNPs were characterized for size, morphology, and surface charge by UV–visible spectroscopy, dynamic light scattering (DLS), and transmission electron microscopy (TEM). The synthesis protocol and characterization studies are described in the [Supporting Information](#). AuNPs were conjugated to a metal-chelating polymer (MCP) pre-complexed to ¹⁷⁷Lu. The MCP was a di-block copolymer with a polyethylene glycol (PEG; 2 kDa) block and a block of polyglutamide with 13 DOTA (1,4,7,10-tetraazacyclododecane-1,4,7,10-tetraacetic acid) chelators for complexing ¹⁷⁷Lu and six lipoic acid [PEG-pGlu(DOTA)₁₃-LA₆] groups that form a stable multivalent gold–thiol bond with AuNPs. The MCP was synthesized as previously reported²⁴ but with modifications. Approximately 3 μg of the MCP was labeled

with 3–6 MBq of $^{177}\text{LuCl}_3$ (McMaster University) at 80 °C for 30 min in 0.1 M sodium acetate buffer, pH 5.5. The ^{177}Lu -MCP was then reacted with 4×10^{11} AuNPs for 1 h at 60 °C in low-binding microcentrifuge tubes (Axygen). ^{177}Lu -AuNPs were purified (>95%) from the unconjugated ^{177}Lu -MCP by centrifugation at 15,000g for 15 min at 4 °C, repeated once.²⁵ The method for measuring the labeling efficiency of the MCP with ^{177}Lu and determining the conjugation efficiency of the ^{177}Lu -MCP to AuNPs and the number of ^{177}Lu -MCP per AuNP are described in the [Supporting Information](#). The cytotoxicity of ^{177}Lu -AuNPs in vitro on U251-Luc cells was measured in a clonogenic survival assay, and DNA double-strand breaks (DSBs) caused by ^{177}Lu were visualized and quantified by confocal immunofluorescence microscopy probing for phosphorylated histone-2AX (γ -H2AX), as described in the [Supporting Information](#).

Human GBM Mouse Xenograft Model. Human GBM tumors were established by stereotaxic inoculation of luciferase-transfected U251-Luc human GBM cells into the right cerebral hemisphere of the brain in female 6–8 week-old NRG mice (Cancer Stem Cell Colony, Princess Margaret Cancer Centre).²⁶ U251-Luc tumors recapitulate the most important histopathologic features of human GBM, especially an infiltrative pattern of invasion and palisading necrosis.²⁷ NRG mice were used to establish U251-Luc tumors and to study the effectiveness and normal tissue toxicity of ^{177}Lu -AuNPs because other immunocompromised strains of mice such as NOD SCID mice harbor the $\text{Prkdc}^{\text{Scid}}$ mutation in DNA repair that results in unusual sensitivity to radiation.²⁸ Luciferase-transfected U251-Luc human GBM cells were provided by Dr. James Rutka (Hospital for Sick Children, Toronto, ON, Canada) and were previously inoculated into the brain in NOD scid gamma (NSG) mice to establish orthotopic human GBM tumors.²⁹ U251-Luc cells were cultured at 37 °C/5% CO_2 in DMEM supplemented with 10% FBS (Gibco-Invitrogen), penicillin (100 U/mL), streptomycin (100 $\mu\text{g}/\text{mL}$), 4 mM glutamine, and 400 μM sodium pyruvate. Mice were anaesthetized with isoflurane 2% in O_2 and positioned in a stereotaxic frame (Stoelting). A small incision was made in the skin to expose the skull, and a burr hole was drilled 2.5 mm lateral and 1.5 mm anterior to the bregma suture. A precision 33-gauge microsyringe (Hamilton) was slowly lowered to 4 mm ventral depth and then retracted to 3.5 mm, and a syringe pump (Stoelting) was used to slowly (0.25 $\mu\text{L}/\text{min}$) inoculate 2×10^5 U251-Luc cells in 5 μL of PBS into the brain. The syringe was then slowly retracted. Bone wax was used to seal the burr hole, and surgical adhesive (Vetbond) was applied to close the incision. Mice received meloxicam (1 mg/kg) s.c. for post-operative analgesia. Animal studies were performed under a protocol (AUP 2780.16) approved by the Animal Care Committee at the University Health Network following Canadian Council on Animal Care (CCAC) guidelines.

Imaging and Biodistribution Studies. At 2 weeks post-inoculation of U251-Luc cells when tumors were ~ 2 mm in diameter, groups of NRG mice ($n = 3$ –4) were anaesthetized with isoflurane 2% in O_2 , and 1–2 MBq (5 μL) of ^{177}Lu -AuNPs (4×10^{11} AuNPs) was stereotaxically infused into the tumor over 20 min by CED at a flow rate of 0.25 $\mu\text{L}/\text{min}$ using a Hamilton syringe and a syringe pump (Stoelting) through the access hole used to inoculate tumor cells. This flow rate is within the range previously studied for CED of other therapeutic agents including other types of NPs in mouse

tumor models of GBM (0.1–10 $\mu\text{L}/\text{min}$).^{14,30} Another group of tumor-bearing mice ($n = 3$ –4) were injected with 1–2 MBq of the ^{177}Lu -MCP (1 μg) not conjugated to AuNPs. Mice were imaged on a nanoScan SPECT/CT/PET tomograph (Mediso) equipped with four NaI(Tl) detectors fitted with 0.85 mm multi-pinhole collimators. Images were acquired using a 256 \times 256 matrix with energy windows centered ($\pm 10\%$) around the 208, 113, and 56 keV γ -photopeaks of ^{177}Lu . CT images were acquired with 50 kVp X-rays, 980 μA , and a 300 ms exposure time. Images were re-constructed and co-registered with Mediso InterView Fusion software (Version 3.09). Images of the head were acquired at 0, 7, 14, and 21 d for ^{177}Lu -AuNPs or at 0, 1, 2, and 3 d for ^{177}Lu -MCPs. Whole-body retention of ^{177}Lu was measured by placing the mouse in a radioisotope dose calibrator (CRC-15R, Capintec) at selected time points up to 16 d post-injection. In a separate study, groups of NRG mice ($n = 3$ –5) infused with ^{177}Lu -AuNPs were sacrificed at 1, 24, 72, 168, or 336 h post-injection. The brain was excised, and samples of blood and other tissues were collected and weighed. The brain was divided into the tumor-bearing right cerebral hemisphere, normal left hemisphere, and cerebellum. ^{177}Lu was measured in a γ -counter (PerkinElmer) and expressed as percent injected dose/g (% ID/g).

Estimation of Radiation Absorbed Doses. The radiation absorbed doses in the brain and other organs in NRG mice after CED of 1.0 MBq of ^{177}Lu -AuNPs were estimated by the Medical Internal Radiation Dose (MIRD) formalism as $D = \sum \tilde{A}_s \times S$, where \tilde{A}_s is the cumulative activity ($\text{Bq} \times \text{s}$) in the source organ and S is the Snyder factor ($\text{Gy Bq}^{-1} \text{s}^{-1}$).³¹ $\tilde{A}_{s(0-336\text{h})}$ was calculated from the area-under-the-curve from 0 to 336 h of a plot of ^{177}Lu (Bq) versus time (s). $\tilde{A}_{s(336\text{h}-\infty)}$ was calculated by dividing the activity at the final measured time point (336 h) by the decay constant of ^{177}Lu ($1.21 \times 10^{-6} \text{s}^{-1}$), thus assuming further elimination only by radioactive decay. ^{177}Lu values in source organs at each time point since the time of injection were calculated by multiplying the % ID/g values from biodistribution studies since the time of injection by the injected dose (set to 1×10^6 Bq) and decay correction factor and by the weight of the source organs (g).³² Published mouse organ S -values for ^{177}Lu were used.³³ The doses per MBq of ^{177}Lu -AuNPs in the tumor, right cerebral hemisphere (excluding the tumor), left cerebral hemisphere, or cerebellum were estimated by the MIRD formalism, except that only these four source/target regions were considered, while doses from other source organs were neglected due to much lower activity and greater distance in comparison to the brain. The activity in the tumor was assumed to account for 90% of total activity in the right cerebral hemisphere. Sixteen S -values for source to target regions were calculated using the Monte Carlo N-Particle program (MCNP 6.1),³⁴ assuming the brain as an elliptic dome divided into the right and left cerebral hemispheres and cerebellum (Supporting Information, [Figure S1](#)). The ellipsoid was centered at 0, 0, 0 with the principle semi-axes of 0.528, 0.594, and 0.639 cm, respectively, estimated based on MRI images of mouse brains. The tumor was assumed to be a 0.2 cm-diameter sphere centered at 0.25, 0.15, and 0.3 cm. ^{177}Lu was assumed to be distributed homogeneously in each source organ. The spectra of β particles, Auger and internal conversion (IC) electrons, X-rays, and γ -rays were taken from the MIRD radionuclide data.³⁵

Evaluation of Normal Tissue Toxicity. Normal tissue toxicity was evaluated in NRG mice ($n = 4$ –5) with U251-Luc

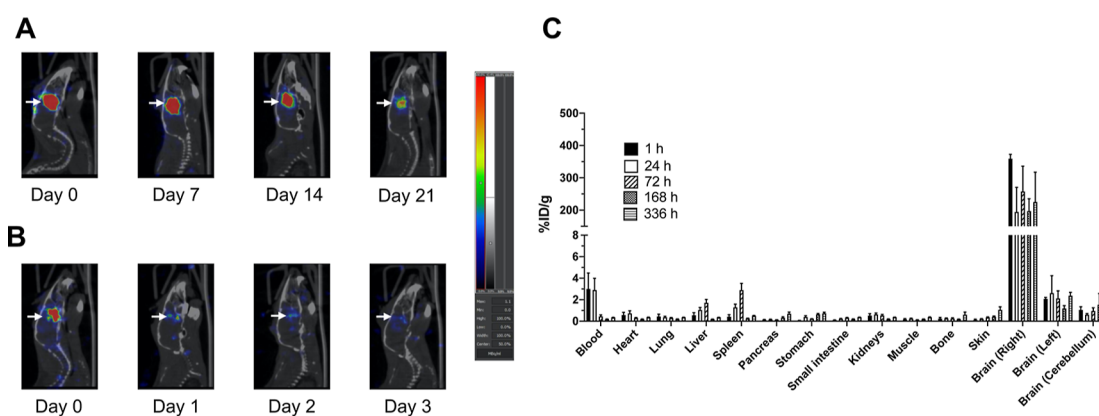


Figure 1. Sagittal SPECT/CT images of an NRG mouse with a U251-Luc human GBM tumor in the right cerebral hemisphere of the brain (arrows) after CED of 1.0 MBq of (A) ^{177}Lu -AuNPs or (B) ^{177}Lu -MCPs (not conjugated to AuNPs). Images were obtained 0, 7, 14, and 21 d post-infusion for ^{177}Lu -AuNPs and 0, 1, 2, and 3 d post-infusion for ^{177}Lu -MCPs. (C) Percent injected dose/g (% ID/g) of ^{177}Lu in the tumor-bearing right cerebral hemisphere, contralateral left hemisphere, or cerebellum and in the blood and other organs at selected times after CED of 1–2 MBq of ^{177}Lu -AuNPs (4×10^{11} AuNPs) in NRG mice. The y-axis was split to more clearly show uptake in organs with low % ID/g.

tumors infused by CED with 1.5 MBq ($5 \mu\text{L}$) of ^{177}Lu -AuNPs (4×10^{11} AuNPs) or normal saline. Body weight was monitored every 2–3 d up to 14 d, and a body weight index (BWI) was calculated by dividing the weight at each time point by the pre-treatment body weight. At 14 d, the mice were sacrificed, and samples of blood were collected into lithium heparin-coated microtubes for biochemistry analyses on Prep Profile II analysis rotors and a VetScan VS2 analyzer (Abaxis). Blood samples were collected into EDTA-coated microtubes for hematology analysis using a VetScan HM5 analyzer (Abaxis).

Treatment of GBM Tumors. Groups of 8–10 NRG mice with orthotopic U251-Luc GBM tumors were treated by CED of 1.1 ± 0.2 MBq ($5 \mu\text{L}$) of ^{177}Lu -AuNPs (4×10^{11} AuNPs). Control mice received unlabeled AuNPs (4×10^{11} AuNPs) or normal saline. Tumor growth was monitored weekly up to 21 d by BLI on an IVIS Spectrum system (PerkinElmer) after intraperitoneal injection of $200 \mu\text{L}$ of D-luciferin (15 mg/mL in PBS). The BLI signal was measured in radiance units (photons/s/cm²/steradian), and a tumor growth index (TGI) was calculated by dividing the BLI signal at each time point by the pre-treatment BLI signal. At 28 d, MRI was performed on an M3 1 Tesla system (Aspect Imaging). The mouse was positioned in the prone position. The head was fixed in place and positioned inside the head coil using a bite bar. High-resolution T2-weighted images were acquired in the coronal plane with a 2D fast spin-echo sequence. The scan parameters were as follows: repetition time 3500 ms; echo time (TE) 80.2 ms; flip angle 90°; in-plane matrix: 240×240 mm; 8 slices; number of excitations: 6; bandwidth: 70 kHz; in-plane pixel size: $0.1953 \text{ mm} \times 0.1953 \text{ mm}$; slice thickness: 1 mm; and acquisition time: 7.42 min. The tumor volume was estimated by determining the tumor margins in each slice, multiplying by the slice thickness, and summing these values. Long-term monitoring of all mice was performed up to 150 d. Mice were sacrificed when they reached a humane endpoint, and Kaplan–Meier survival curves were constructed by plotting the proportion of surviving mice versus time post-treatment (d). Body weight was monitored, and a BWI was calculated as described earlier and plotted versus time. H&E staining was performed on the brain ex vivo following sacrifice at the humane endpoint to detect the presence of tumor and assess any radiation necrosis of normal brain tissue.

Statistical Analysis. Results were expressed as mean \pm SEM. Statistical significance was tested by ANOVA ($P < 0.05$). Statistical comparisons of Kaplan–Meier median survival between treated and control mice were made using the log–rank (Mantel–Cox) test ($P < 0.05$).

RESULTS

Synthesis and Characterization of ^{177}Lu -AuNPs and Cytotoxicity In Vitro. Spherical AuNPs (mean diameter 23 ± 3 nm) were synthesized and conjugated to multiple (197 ± 36) MCPs pre-complexed with ^{177}Lu (Supporting Information, Figure S2). High temperature ($80 \text{ }^\circ\text{C}$) and high concentrations of MCPs ($\sim 1 \mu\text{g}/\mu\text{L}$) and $^{177}\text{LuCl}_3$ ($\sim 1 \text{ MBq}/\mu\text{L}$) in 0.1 M sodium acetate buffer, pH 5.5, were required to achieve high labeling efficiency of the MCP ($92 \pm 5\%$) for subsequent conjugation to AuNPs. Direct labeling of MCP-conjugated AuNPs with ^{177}Lu proved not feasible due to low labeling efficiency. The hydrodynamic diameter of MCP-conjugated AuNPs by DLS was 29 nm, and the surface charge was -17.8 mV. Treatment of U251-Luc cells in vitro with ^{177}Lu -AuNPs (2.0 MBq , 4×10^{11} AuNPs) in 1 mL medium for 16 h reduced the clonogenic survival to 0.005 ± 0.002 (Supporting Information, Figure S3A), which was associated with a 14.3-fold significant increase in DNA DSBs in the nucleus of U251-Luc cells compared to untreated cells, measured by immunofluorescence microscopy probing for γH2AX (Figure S3B,C). Details of these studies are provided in the Supporting Information.

Imaging and Biodistribution Studies. SPECT/CT images of an NRG mouse with a U251-Luc tumor in the brain that administered ^{177}Lu -AuNPs by CED showed localization and retention of radioactivity confined to the infusion site up to 21 d (Figure 1A). In contrast, a mouse infused with ^{177}Lu -MCPs not conjugated to AuNPs showed rapid elimination of radioactivity from the brain with little remaining at 2–3 d (Figure 1B). Uptake of ^{177}Lu -AuNPs in other regions of the brain or peripheral organs outside the brain was not visualized (Figure 1A and Supporting Information, Figure S4). Radioactive decay was responsible for the decreased signal in the brain at 21 d post-injection of ^{177}Lu -AuNPs. Mice infused with ^{177}Lu -MCP exhibited rapid elimination of activity with $<5\%$ remaining in the body at 15 d,

while >77% of activity in mice infused with ^{177}Lu -AuNPs remained at 15 d (Supporting Information, Figure S5). Biodistribution studies of ^{177}Lu -AuNPs (Figure 1C) revealed high radioactivity in the tumor-bearing right cerebral hemisphere at 1 h ($359.1 \pm 13.5\%$ ID/g) and no significant decrease up to 336 h post-injection ($225.2 \pm 92.3\%$ ID/g; $P > 0.05$). In contrast, uptake in the contralateral left cerebral hemisphere or cerebellum was 171-fold and 360-fold significantly lower, respectively, at 1 h ($2.1 \pm 0.1\%$ ID/g and $1.0 \pm 0.3\%$ ID/g, respectively; $P \leq 0.0001$) and remained low with no significant change up to 336 h ($2.4 \pm 0.3\%$ ID/g; $P > 0.05$ and $2.3 \pm 0.5\%$ ID/g; $P > 0.05$). ^{177}Lu in the blood was $3.0 \pm 1.5\%$ ID/g at 1 h post-infusion but non-significantly decreased to $0.3 \pm 0.0\%$ ID/g at 336 h ($P > 0.05$), while liver and spleen uptake increased from $0.6 \pm 0.2\%$ ID/g and $0.4 \pm 0.2\%$ ID/g, respectively, at 1 h to $1.7 \pm 0.3\%$ ID/g and $2.9 \pm 0.6\%$ ID/g at 72 h, respectively ($P > 0.05$). Liver and spleen activity decreased to $0.3 \pm 0.0\%$ ID/g and $0.5 \pm 0.0\%$ ID/g, respectively, at 336 h ($P > 0.05$). There was <2% ID/g in all other normal organs at any time point.

Estimation of Radiation Absorbed Doses. The radiation absorbed doses in the tumor, brain, and other organs in NRG mice receiving CED of 1.0 MBq of ^{177}Lu -AuNPs (4×10^{11} AuNPs) are shown in Table 1. The tumor doses were high

Table 1. Radiation Absorbed Doses in NRG Mice with Orthotopic U251-Luc Human GBM Tumors Receiving CED of ^{177}Lu -AuNPs^a

organ/region	absorbed dose (Gy)
heart	0.08 ± 0.01
lungs	0.06 ± 0.01
liver	0.15 ± 0.03
spleen	0.22 ± 0.05
pancreas	0.07 ± 0.02
stomach	0.09 ± 0.02
intestine	0.05 ± 0.01
kidneys	0.08 ± 0.01
carcass	0.03 ± 0.01
whole brain ^b	16.2 ± 5.8
cerebellum ^c	0.22 ± 0.05
left cerebral hemisphere (non-tumor bearing) ^c	0.3 ± 0.1
right cerebral hemisphere (excluding tumor) ^{c,d}	6.4 ± 3.3
tumor ^{c,d}	599 ± 311

^aMice received CED of 1.0 MBq of ^{177}Lu -AuNPs (4×10^{11} AuNPs).

^bMean absorbed dose for the whole brain calculated by summing the radioactivity from the left and right cerebral hemispheres and cerebellum and treating the brain as a single source or target organ.

^cOnly the cerebellum and left and right cerebral hemispheres of the brain and tumor were considered as source and target regions. ^dThe size of the tumor was 0.2 cm diameter and was situated in the right cerebral hemisphere of the brain (Supporting Information, Figure S1).

(599 ± 311 Gy). Doses were 93-fold lower in the normal right cerebral hemisphere excluding the tumor (6.4 ± 3.3 Gy) and 1997-fold lower in the contralateral normal left cerebral hemisphere (0.3 ± 0.1 Gy) and 2995-fold lower in the cerebellum (0.2 ± 0.1 Gy). The tumor doses were 3000–4000-fold higher than those in the spleen (0.22 ± 0.05 Gy) or liver (0.15 ± 0.03 Gy). The absorbed doses in all other normal organs were <0.1 Gy.

Evaluation of Normal Tissue Toxicity. There was only a minor decrease (<2%) in the BWI in NRG mice after CED of 1.5 MBq of ^{177}Lu -AuNPs (4×10^{11} AuNPs) at 6 to 10 d which

recovered at 14 d compared to control mice receiving normal saline (Figure 2). There were no significant differences in blood biochemistry or hematology values at 14 d after infusion of ^{177}Lu -AuNPs or normal saline (Table 2).

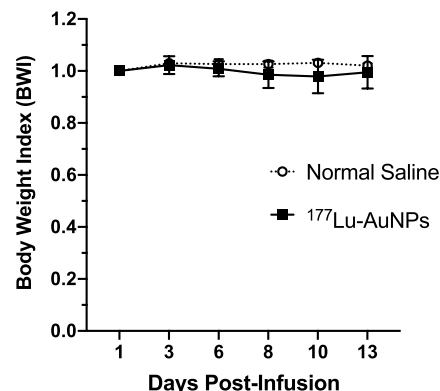


Figure 2. BWI vs time in NRG mice with U251-Luc human GBM tumors after CED of 1.5 MBq of ^{177}Lu -AuNPs (4×10^{11} AuNPs) or normal saline.

Table 2. Blood Biochemistry and Hematology at 14 d Post-CED of ^{177}Lu -AuNPs or Normal Saline in NRG Mice with Orthotopic U251-Luc Human GBM Tumors^a

parameter ^b	^{177}Lu -AuNPs	normal saline
ALT (U/L)	27.0 ± 2.9	19.8 ± 1.7
CRE ($\mu\text{mol/L}$)	18.0 ± 0.0	18.3 ± 0.5
GLU (mmol/L)	8.5 ± 4.2	12.6 ± 1.3
TP (g/L)	45.0 ± 2.1	47.3 ± 2.6
ALP (U/L)	55.8 ± 6.3	61.0 ± 6.4
BUN (mmol/L)	7.2 ± 1.5	8.2 ± 0.4
HGB (g/dL)	12.1 ± 1.4	13.1 ± 0.6
HCT (%)	38.0 ± 1.3	38.2 ± 1.2
RBC ($\times 10^{12}/\text{L}$)	8.6 ± 0.3	8.7 ± 0.3
WBC ($\times 10^9/\text{L}$)	2.4 ± 2.9	0.9 ± 0.3
PLT ($\times 10^9/\text{L}$)	428.3 ± 166.1	441.3 ± 227.8

^aMice received CED of 1.5 MBq ($5 \mu\text{L}$) of ^{177}Lu -AuNPs (4×10^{11} AuNPs) or normal saline ($5 \mu\text{L}$). $n = 4-5$. ^bALT: alanine aminotransferase; CRE: creatinine; GLU: glucose; TP: total protein; ALP: alkaline phosphatase; BUN: blood urea nitrogen; HGB: hemoglobin; HCT: hematocrit; RBC: red blood cells; WBC: white blood cells; and PLT: platelets. No significant differences ($P > 0.05$) were found in any of these parameters for mice receiving ^{177}Lu -AuNPs or normal saline.

Treatment of GBM Tumors. There was a strong BLI signal at the tumor site in the brain in all mice except one at 21 d post-infusion of normal saline (Figure 3A) and in all mice infused with unlabeled AuNPs (Figure 3B). Only one mouse treated with 1.1 ± 0.2 MBq of ^{177}Lu -AuNPs (4×10^{11} AuNPs) showed a minor signal in the brain, while all other mice showed no signal (Figure 3C). The TGI as measured by BLI increased rapidly and exponentially over 21 d in mice receiving normal saline or unlabeled AuNPs but was negligible over this time period for mice treated with ^{177}Lu -AuNPs (Figure 3D). At 21 d, the TGI for mice treated with ^{177}Lu -AuNPs (0.06 ± 0.04) was >700-fold significantly smaller than in mice treated with unlabeled AuNPs (42.8 ± 10.5 ; $P = 0.005$) and 1000-fold lower than in mice infused with normal saline (61.4 ± 27.0 ; $P < 0.005$; Figure 3D).

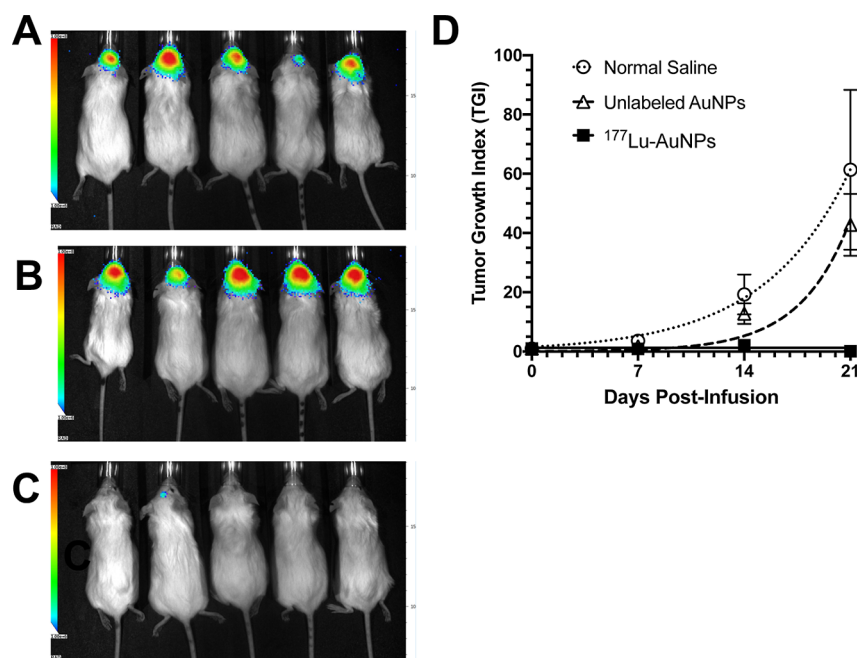


Figure 3. Representative BLI images (radiance in photons/s/cm²/steradian scale: 1×10^6 in blue to 1×10^8 in red) in NRG mice with U251-Luc human GBM tumors at 21 d after CED of (A) normal saline, (B) unlabeled AuNPs (4×10^{11} AuNPs), or (C) 1.1 ± 0.2 MBq of ¹⁷⁷Lu-AuNPs (4×10^{11} AuNPs). (D) TGI vs time (days post-infusion) measured by BLI. Values shown are the mean \pm SEM ($n = 8-10$).

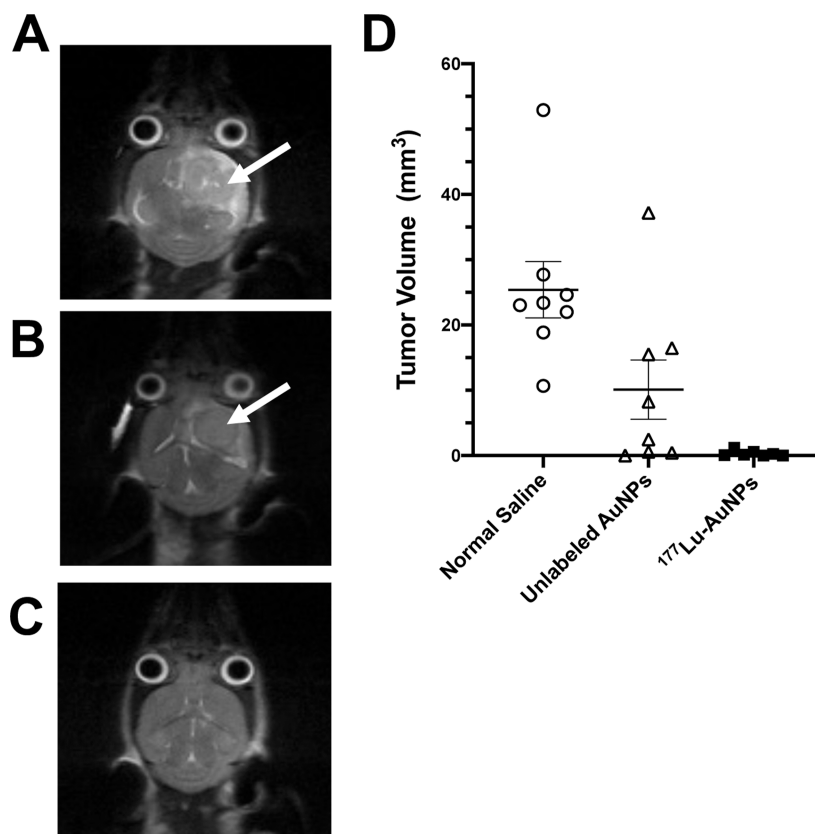


Figure 4. Representative T2-weighted MRI images in NRG mice with U251-Luc human GBM tumors at 28 d after CED of (A) normal saline, (B) unlabeled AuNPs (4×10^{11} AuNPs), or (C) 1.1 MBq of ¹⁷⁷Lu-AuNPs (4×10^{11} AuNPs). Tumors in the brain in control mice are indicated by the arrows. There was no visible tumor in the brain in mice treated with ¹⁷⁷Lu-AuNPs. (D) Tumor volume measured by analysis of MRI images. Horizontal lines indicate the mean \pm SEM ($n = 8-10$).

T2-weighted MRI at 28 d post-infusion of ¹⁷⁷Lu-AuNPs revealed no evidence of tumor in the brain, while control mice

treated with unlabeled AuNPs or normal saline showed large tumors (Figure 4A–C). Closer analysis of the MRI images

revealed that there were very small tumors in 9/10 mice at 28 d after treatment with ^{177}Lu -AuNPs, but the mean tumor volume was $0.33 \pm 0.17 \text{ mm}^3$, which was 77-fold smaller than in control mice receiving normal saline ($25.4 \pm 4.3 \text{ mm}^3$; $P \leq 0.001$) (Figure 3D). Tumors in mice treated with unlabeled AuNPs were 2.5-fold smaller ($10.1 \pm 4.5 \text{ mm}^3$) than normal saline-treated mice, but this difference was not significant ($P > 0.05$).

Long-term monitoring (Figure 5A) revealed that 5/8 mice (62.5%) treated with ^{177}Lu -AuNPs survived up to 150 d, while

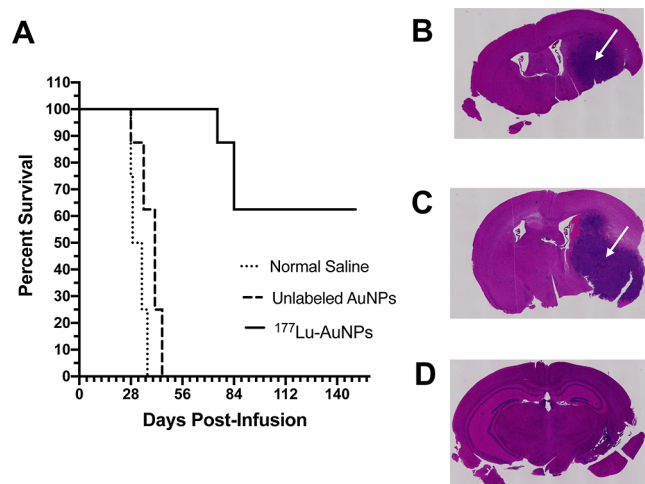


Figure 5. (A) Kaplan–Meier survival plot for NRG mice with U251-Luc human GBM tumors treated by CED of $1.1 \pm 0.2 \text{ MBq}$ of ^{177}Lu -AuNPs (4×10^{11} AuNPs), unlabeled AuNPs (4×10^{11} AuNPs), or normal saline. H&E staining of the brain in representative mice infused with (B) normal saline, (C) unlabeled AuNPs, or (D) ^{177}Lu -AuNPs. Large GBM tumors are shown in control mice (arrow in panels B and C) but not in the mouse treated with ^{177}Lu -AuNPs (panel D).

8/8 control mice (100%) treated with unlabeled AuNPs reached a humane endpoint requiring sacrifice by 45 d (median survival = 41 d) and 8/8 control mice (100%) receiving normal saline required sacrifice by 39 d (median survival = 31 d). There was no significant difference (Log–Rank test; $P > 0.05$) in median survival for mice treated with unlabeled AuNPs compared to mice receiving normal saline. One of the mice treated with ^{177}Lu -AuNPs that reached the humane end-point early was the mouse that exhibited a small BLI signal in the brain (Figure 3C). H&E staining of the brain revealed large tumors in control mice treated with normal saline (Figure 5B) or unlabeled AuNPs (Figure 5C), but there is no histological evidence of tumor in mice treated with ^{177}Lu -AuNPs (Figure 5D).

The BWI increased with time in mice treated with ^{177}Lu -AuNPs, indicating good health, but decreased by almost 20% in control mice treated with unlabeled AuNPs or normal saline, indicating poor health (Figure 6A). H&E staining of the brain in a mouse treated with ^{177}Lu -AuNPs revealed no evidence of radiation necrosis in the margin surrounding residual tumor in the right cerebral hemisphere (Figure 6B). Similarly, in a separate mouse treated with ^{177}Lu -AuNPs, there was no evidence of radiation necrosis in the contralateral left cerebral hemisphere (Figure 6C).

DISCUSSION

We report here highly effective treatment of orthotopic U251-Luc human GBM tumors in the brain in NRG mice by CED of AuNPs labeled with β -particle-emitting ^{177}Lu without evidence of normal tissue toxicity including to the normal brain. Other NPs, for example, ^{186}Re -labeled liposomes, ^{151}Re -labeled lipid nanocapsules,¹⁷ or ^{177}Lu -labeled metallofullerenes,²⁰ administered by CED have been previously studied for treatment of human GBM tumors, but our report is the first to describe treatment of GBM tumors in mice by CED of ^{177}Lu -AuNPs. CED circumvented the BBB, which is a major obstacle to delivery of NPs into the brain following i.v. injection.³⁶ A meta-analysis of 36 preclinical studies reported that only 0.06% ID/g of i.v. injected AuNPs in mice were taken up into the brain.³⁷ In contrast, we achieved a 4000–6000-fold higher concentration of ^{177}Lu -AuNPs (225–359% ID/g) in GBM tumors in NRG mice when administered by CED (Figure 1C). Moreover, the BBB may pose a barrier to redistribution of ^{177}Lu -AuNPs from the brain to peripheral organs outside the brain.³⁸ SPECT/CT images and biodistribution studies showed that ^{177}Lu -AuNPs were confined to the infusion site in the right cerebral hemisphere of the brain up to 21 d with minimal redistribution to other brain regions or organs outside the brain (Figure 1A,C and Supporting Information, Figure S4). In contrast, CED of ^{177}Lu -MCPs not conjugated to AuNPs showed elimination from the brain (Figure 1B) and from the body over 2–3 d (Supporting Information, Figure S5). In a previous report,²⁴ we found that >90% of radioactivity in mice injected i.v. with ^{177}Lu -MCPs not bound to AuNPs was eliminated into the urine over 6 h, indicating that unconjugated ^{177}Lu -MCPs were eliminated renally. In the current study, we synthesized ^{177}Lu -AuNPs with a mean diameter of $23 \pm 3 \text{ nm}$, which was similar to 30 nm-diameter ^{177}Lu -AuNPs²² or ^{111}In -AuNPs³⁹ injected intratumorally for treatment of s.c. BC tumors in mice. The optimal size of ^{177}Lu -AuNPs for CED into the brain for treatment of GBM is not known, but it is possible that smaller AuNPs may diffuse more homogeneously at the infusion site in the brain than larger AuNPs. It is difficult to compare results in different tumor models, but retention of ^{177}Lu -AuNPs after CED into the brain reported here appears greater than that previously reported for other radiolabeled NPs administered by CED in GBM tumor models. Wilson et al. reported that only 20% of ^{177}Lu -metallofullerenes infused by CED in mice with U87MG human GBM tumors remained in the brain at 24 h.²⁰ Phillips et al. found that ~50% of $^{99\text{m}}\text{Tc}$ -liposomes were retained in the brain of rats with U87MG xenografts after CED, with some redistribution to the cerebellum and brainstem, depending on the volume of infusion.¹⁵ Cikankowitz et al. reported that ~70% of ^{188}Re -labeled lipid nanocapsules administered by CED were retained in the brain of nude mice with Lab1 human glioma tumors.⁴⁰ In our study, the uptake of ^{177}Lu -AuNPs in most normal tissues outside the brain was very low (<0.2% ID/g), except for the liver and spleen which was 2–3% ID/g at 72 h, but these decreased to <0.5% ID/g at 336 h (Figure 1C). Our results agree with those reported by Bobyk et al., who showed by CT imaging that unlabeled AuNPs (15 nm diameter) administered by CED were retained in the brain in rats with orthotopic glioma tumors up to 14 d.⁴¹ The mechanism of retention of ^{177}Lu -AuNPs in the brain is not known but may be due to physical entrapment of the AuNPs or possibly phagocytosis by

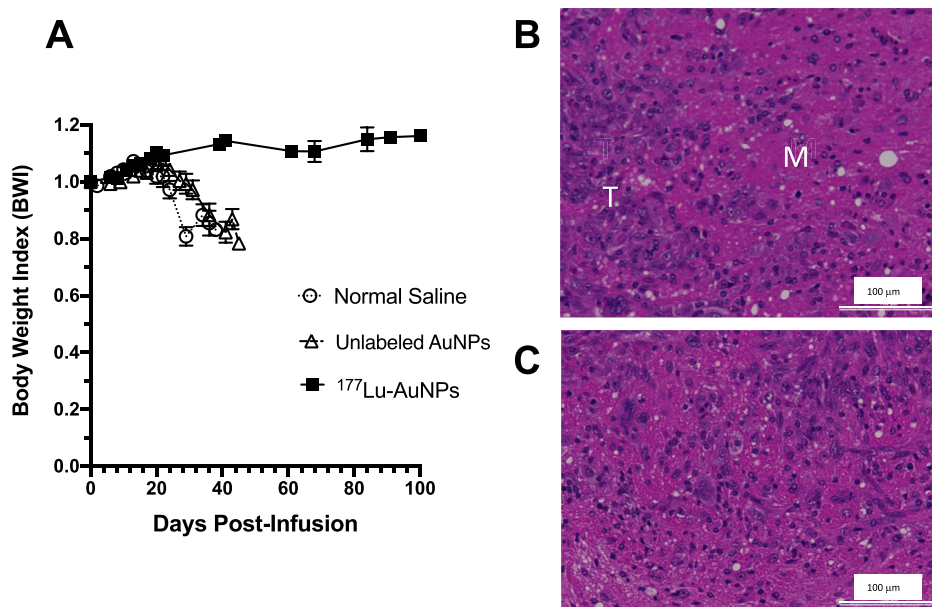


Figure 6. (A) BWI vs time (days post-infusion) in NRG mice with U251-Luc human GBM tumors treated by CED of 1.1 ± 0.2 MBq of ^{177}Lu -AuNPs (4×10^{11} AuNPs), unlabeled AuNPs (4×10^{11} AuNPs), or normal saline. (B) H&E-stained section (magnification $20\times$) of the right cerebral hemisphere of the brain in a mouse treated with ^{177}Lu -AuNPs revealing the residual tumor (T) and the surrounding margin (M). (C) H&E-stained section of the normal left cerebral hemisphere of the brain in a mouse treated with ^{177}Lu -AuNPs. There was no evidence of radiation necrosis of the normal brain.

immune cells infiltrating the tumor as suggested for other NPs administered by CED.¹⁴

High radiation absorbed doses in the tumor (599 Gy) were estimated after CED of 1.0 MBq of ^{177}Lu -AuNPs in NRG mice with U251-Luc tumors (Table 1). Due to the maximum 1.8 mm range of the moderate energy β -particles ($E\beta_{\text{max}} = 0.497$ MeV) emitted by ^{177}Lu ,¹⁶ these tumor doses were highly conformal, with 93-fold lower doses calculated for the normal right cerebral hemisphere of the brain excluding the tumor (6.4 Gy) and 2000–3000-fold lower doses in the contralateral left hemisphere (0.3 Gy) or cerebellum (0.2 Gy). The doses in all peripheral organs were <0.1 Gy. Philips et al. reported that the doses for ^{186}Re -liposomes administered by CED in rats with human GBM tumors were high, ranging from 220 to 1845 Gy, depending on the amount of ^{186}Re ,¹⁵ but no information was reported on the conformity of the doses around the tumor. The dosimetry modeling in our study (Supporting Information, Figure S1 and Table 1) for the first time provides insights into the high spatial conformity of the radiation absorbed dose in the tumor from CED of ^{177}Lu -AuNPs. The tumor dose delivered by ^{177}Lu -AuNPs was 100-fold higher than the total radiation dose delivered by standard-of-care external radiation treatment of GBM (50–60 Gy in fractionated doses).⁴²

No normal tissue toxicity was observed at 14 d post-injection of 1.5 MBq ^{177}Lu -AuNPs (4×10^{11} AuNPs) in NRG mice (Table 2). No change in the health of mice treated with ^{177}Lu -AuNPs was noted, and there was no significant decrease in body weight compared to control mice treated with normal saline (Figures 2 and 6A). Toxicity to the brain, if manifested, may be caused by the β -particle emissions of ^{177}Lu or by the AuNPs. External radiotherapy of GBM is limited to a total of 60 Gy in fractionated doses due to toxicity on the normal brain.⁴² However, as discussed, the tumor doses deposited by ^{177}Lu -AuNPs are highly conformal, with almost 100-fold lower doses estimated for the normal right hemisphere of the brain excluding the tumor (6.4 Gy) and 2000–3000-fold lower

doses (0.2–0.3 Gy) in more distant regions of the brain (Table 1). These radiation doses in the normal brain would not be expected to be harmful based on the total doses of radiation used safely for treatment of GBM. The incidence of radiation necrosis in the brain in humans over 1–2 years after radiation treatment is predicted to be 5% at a total dose of 120 Gy and 10% at a dose of 150 Gy, when administered as fractionated doses <2.5 Gy.⁴³ The doses to the normal brain in mice in our study were 20-fold to 600-fold lower than these minimum doses causing serious radiation toxicity in humans; thus, we do not anticipate toxicity from the β -particle emissions of ^{177}Lu in the brain. In future studies, we plan to construct more detailed radiation dose maps for ^{177}Lu -AuNPs administered by CED to NRG mice with U251-Luc tumors to precisely map the doses in the tumor and surrounding normal brain. It is important to appreciate that in a human, CED of ^{177}Lu -AuNPs into a tumor is expected to deposit much lower doses in the normal brain than in a mouse, due to the greater distances between ^{177}Lu -AuNPs infused into the tumor and distant brain regions, relative to the short maximum 1.8 mm pathlength of the β -particles emitted by ^{177}Lu . Histopathological examination by H&E staining of the tumor margin in the right cerebral hemisphere in a mouse treated with ^{177}Lu -AuNPs or in the contralateral normal left cerebral hemisphere of the brain in another treated mouse at 10 weeks post-infusion of ^{177}Lu -AuNPs did not show signs of radiation necrosis (Figure 6B,C, respectively). Histopathological changes associated with radiation necrosis in the brain in mice and humans are evidenced by tissue edema, necrosis, decreased cellularity, extravasation of blood around telangiectatic blood vessels, and fibrinoid vascular necrosis.⁴⁴

The absence of normal tissue toxicity from ^{177}Lu -AuNPs administered by CED in NRG mice agrees with the minimal toxicity reported for treatment of GBM tumors in rats by CED of ^{186}Re -liposomes.¹⁵ ^{186}Re emits higher energy β -particles than ^{177}Lu ($E\beta_{\text{max}} = 1.08$ vs 0.497 MeV) that have a longer range in

tissues (4.8 vs 1.8 mm).¹⁶ Thus, the radiation doses from ¹⁷⁷Lu would be more conformal than those of ¹⁸⁶Re, which should render ¹⁷⁷Lu-AuNPs less harmful than ¹⁸⁶Re-liposomes to the normal brain and other tissues outside the brain. Only a few studies have examined the toxicity of unlabeled AuNPs infused directly into the brain. Bobyk et al. reported no signs of toxicity, that is, seizure, lethargy, hemiparesis, or weight loss (>5%) in rats over a 30 d period after CED into the brain of <250 μg (7×10^{12}) of 15 nm AuNPs or <50 μg (6×10^{14} AuNPs) of 2 nm AuNPs, but higher amounts of 2 nm AuNPs were toxic.⁴¹ Lira-Diaz et al. reported a transient microgliosis but no major toxicity in mice intracerebrally injected with 8.5×10^9 AuNPs (8 nm).⁴⁵ In our study, we treated tumor-bearing NRG mice with CED of 4×10^{11} ¹⁷⁷Lu-AuNPs (23 nm), which corresponds to ~50 μg in a 20 g mouse (2500 μg/kg). The absence of normal tissue toxicity for this mass and size of ¹⁷⁷Lu-AuNPs (Table 2 and Figures 2 and 6A) is consistent with these previous toxicity studies of AuNPs administered into the brain.

Remarkable results were achieved by treatment of NRG mice with U251-Luc tumors by CED of 1.1 ± 0.2 MBq of ¹⁷⁷Lu-AuNPs (4×10^{11} AuNPs). Only one treated mouse exhibited a minor BLI signal in the brain, while all other mice showed no signal at 21 d post-CED of ¹⁷⁷Lu-AuNPs (Figure 3C). All control mice receiving unlabeled AuNPs (Figure 3B) and all mice except one receiving normal saline (Figure 3A) showed an intense BLI signal, indicating the presence of tumor in the brain. Mice treated with ¹⁷⁷Lu-AuNPs exhibited almost complete tumor growth arrest by BLI, while tumors grew rapidly and exponentially in mice treated with unlabeled AuNPs or normal saline (Figure 3D). Moreover, MRI showed no visible tumor in the brain at 28 d in mice treated with ¹⁷⁷Lu-AuNPs (Figure 4C), while mice treated with unlabeled AuNPs (Figure 4B) or normal saline (Figure 4A) showed large tumors. Tumor size measured by MRI was reduced by >77-fold in mice treated with ¹⁷⁷Lu-AuNPs compared to mice receiving normal saline (Figure 4D). BLI and MRI are sensitive for detecting GBM tumors in the brain in mice, and imaging results from these two modalities are usually well-correlated.⁴⁶ BLI is convenient and sensitive for monitoring tumor growth versus time, while MRI has high spatial resolution and allows accurate measurement of tumor volume.

Treatment with ¹⁷⁷Lu-AuNPs prolonged the survival of 5/8 (62.5%) mice for over 150 d post-CED, which is at least a 3.3- and 3.8-fold significant increase in median survival compared to mice receiving unlabeled AuNPs or normal saline (Figure 5A). Since over half of the ¹⁷⁷Lu-AuNP-treated mice were still healthy and did not reach the humane endpoint at the end of the study which was 150 d post CED, we conservatively estimated the median survival as 150 d. However, tumors in 3/8 mice treated with ¹⁷⁷Lu-AuNPs recurred, causing these mice to reach a humane endpoint at earlier times requiring sacrifice (Figure 5A). One of these mice which reached an early humane end point was the same mouse that showed a small BLI signal in the brain post-treatment with ¹⁷⁷Lu-AuNPs (Figure 3C). The tumor growth-inhibitory properties of ¹⁷⁷Lu-AuNPs observed in vivo were mediated by the β-particle emissions of ¹⁷⁷Lu, which decreased the clonogenic survival of U251-Luc cells exposed to ¹⁷⁷Lu-AuNPs in vitro and caused multiple DNA DSBs in these cells detected by confocal immunofluorescence microscopy probing for γH2AX (Supporting Information, Figure S3).

Body weight increased slightly in mice treated with ¹⁷⁷Lu-AuNPs, which may reflect a low tumor burden and the better health of these mice, while mice treated with unlabeled AuNPs or normal saline lost weight, indicating poor health due to large GBM tumors (Figure 6A). The administered activity of ¹⁷⁷Lu-AuNPs (1.1 ± 0.2 MBq) selected for treatment was based on a previous report in which a range of activities (0.25–1.35 MBq) of ¹⁷⁷Lu-labeled metallofullerenes were administered by CED to mice with orthotopic U87MG tumors and 1.35 MBq was found to be the most effective for increasing survival.²⁰ In addition, a slightly higher administered activity of ¹⁷⁷Lu-AuNPs (1.5 MBq; 4×10^{11} AuNPs) was safe in toxicity studies (Table 2). There were also practical considerations in infusing ¹⁷⁷Lu-AuNPs by CED into the brain in mice, in that the volume was limited to ~5 μL, and this affected the amount of ¹⁷⁷Lu-AuNPs that could be administered. Nonetheless, the absence of normal tissue toxicity with ¹⁷⁷Lu-AuNPs suggests that the administered activity could be increased to minimize the risk of tumor recurrence. Furthermore, ¹⁷⁷Lu-AuNPs could be combined with other treatments for GBM including external radiation and temozolomide chemotherapy to further decrease the risk for recurrence. Ultimately, we envision that CED of ¹⁷⁷Lu-AuNPs could be applied to treat residual tumor at the surgical margins to prevent recurrence of GBM after standard-of-care treatments in order to improve patient outcome.

CONCLUSIONS

We conclude that CED of ¹⁷⁷Lu-AuNPs was highly effective for treating U251-Luc human GBM tumors in the brain in NRG mice at amounts that did not cause toxicity to normal tissues. The tumor-growth inhibitory effects of ¹⁷⁷Lu-AuNPs were mediated by the β-particle emissions of ¹⁷⁷Lu, which decreased the clonogenic survival of U251-Luc cells in vitro by causing multiple DNA DSBs. The absence of toxicity to normal tissues from ¹⁷⁷Lu-AuNPs was due to confinement at the site of infusion in the brain combined with the maximum 1.8 mm range of the β-particles, which resulted in a highly conformal radiation absorbed dose around the tumor. These ¹⁷⁷Lu-AuNPs hold great promise for treating patients with GBM to prevent recurrence and improve outcome.

ASSOCIATED CONTENT

Supporting Information

The Supporting Information is available free of charge at <https://pubs.acs.org/doi/10.1021/acs.molpharmaceut.2c00815>.

Methods and results for synthesis and characterization in vitro of AuNPs, conjugation to MCPs for complexing ¹⁷⁷Lu, evaluation of cytotoxicity on U251-Luc cells in vitro by clonogenic assay and measurement of DNA DSBs by confocal immunofluorescence for γH2AX, model for estimation of the radiation absorbed doses in GBM tumors and normal brain regions by MCNP simulation, whole body SPECT/CT images of NRG mice after CED of ¹⁷⁷Lu-AuNPs, and whole body retention of radioactivity in NRG mice after CED of ¹⁷⁷Lu-MCPs or ¹⁷⁷Lu-AuNPs (PDF)

AUTHOR INFORMATION

Corresponding Author

Raymond M. Reilly – Department of Pharmaceutical Sciences, Leslie Dan Faculty of Pharmacy, University of Toronto,

Toronto, Ontario M5S 3M2, Canada; Department of Medical Imaging, Temerty Faculty of Medicine, University of Toronto, Toronto, Ontario M5S 1A8, Canada; Joint Department of Medical Imaging and Princess Margaret Cancer Centre, University Health Network, Toronto, Ontario M5G 2C1, Canada; orcid.org/0000-0003-1038-7993; Email: raymond.reilly@utoronto.ca

Authors

Constantine J. Georgiou – Department of Pharmaceutical Sciences, Leslie Dan Faculty of Pharmacy, University of Toronto, Toronto, Ontario M5S 3M2, Canada;

orcid.org/0000-0002-0602-9416

Zhongli Cai – Department of Pharmaceutical Sciences, Leslie Dan Faculty of Pharmacy, University of Toronto, Toronto, Ontario M5S 3M2, Canada; orcid.org/0000-0002-8937-4943

Noor Alsadon – Department of Pharmaceutical Sciences, Leslie Dan Faculty of Pharmacy, University of Toronto, Toronto, Ontario M5S 3M2, Canada

Hyoungun Cho – Department of Chemistry, University of Toronto, Toronto, Ontario M5S 3H6, Canada

Minou Behboudi – Department of Pharmaceutical Sciences, Leslie Dan Faculty of Pharmacy, University of Toronto, Toronto, Ontario M5S 3M2, Canada

Mitchell A. Winnik – Department of Chemistry, University of Toronto, Toronto, Ontario M5S 3H6, Canada;

orcid.org/0000-0002-2673-2141

James T. Rutka – Division of Neurosurgery, The Hospital for Sick Children, Toronto, Ontario M5G 1X8, Canada; Division of Neurosurgery, Department of Surgery, Temerty Faculty of Medicine, University of Toronto, Toronto, Ontario M5T 1P5, Canada

Complete contact information is available at:

<https://pubs.acs.org/10.1021/acs.molpharmaceut.2c00815>

Notes

The authors declare the following competing financial interest(s): R.M.R. was a speaker at the annual research symposium of the Brain Tumor Foundation of Canada on October 3, 2020 and an invited speaker to the World Gold Council on October 7, 2021. The authors declare that they have no other conflicts/competing interests.

ACKNOWLEDGMENTS

This study was supported by grants from the Brain Tumor Foundation of Canada, the Canadian Cancer Society (CCS), and the Natural Sciences and Engineering Research Council of Canada (NSERC). Funds were donated to the CCS by the World Gold Council in support of this research. C.J.G. was a scholar of the Terry Fox Foundation Strategic Training and Transdisciplinary Radiation Science for the 21st Century (STARS21) program. C.J.G. was also supported by the NSERC Polymer Nanoparticles for Drug Delivery (POND) Collaborative Research and Training Experience (CREATE) program and a MDS Nordion Graduate Scholarship in Radiopharmaceutical Sciences. N.A. was supported by a fellowship from the Precision Medicine Initiative (PRiME) at the University of Toronto.

REFERENCES

- (1) Oronsky, B.; Reid, T. R.; Oronsky, A.; Sandhu, N.; Knox, S. J. A Review of Newly Diagnosed Glioblastoma. *Front Oncol* **2020**, *10*, 574012.
- (2) Delgado-López, P. D.; Corrales-García, E. M. Survival in glioblastoma: a review on the impact of treatment modalities. *Clin. Transl. Oncol.* **2016**, *18*, 1062–1071.
- (3) Stupp, R.; Mason, W. P.; van den Bent, M. J.; Weller, M.; Fisher, B.; Taphoorn, M. J.; Belanger, K.; Brandes, A. A.; Marosi, C.; Bogdahn, U.; et al. Radiotherapy plus concomitant and adjuvant temozolomide for glioblastoma. *N. Engl. J. Med.* **2005**, *352*, 987–996.
- (4) Wallner, K. E.; Galicich, J. H.; Krol, G.; Arbit, E.; Malkin, M. G. Patterns of failure following treatment for glioblastoma multiforme and anaplastic astrocytoma. *Int. J. Radiat. Oncol., Biol., Phys.* **1989**, *16*, 1405–1409.
- (5) Luo, H.; Shusta, E. V. Blood-brain barrier modulation to improve glioma drug delivery. *Pharmaceutics* **2020**, *12*, 1085.
- (6) de Gooijer, M. C.; de Vries, N. A.; Buckle, T.; Buil, L. C. M.; Beijnen, J. H.; Boogerd, W.; van Tellingen, O. Improved brain penetration and antitumor efficacy of temozolomide by inhibition of ABCB1 and ABCG2. *Neoplasia* **2018**, *20*, 710–720.
- (7) Dong, X. Current strategies for brain drug delivery. *Theranostics* **2018**, *8*, 1481–1493.
- (8) D'Amico, R. S.; Aghi, M. K.; Vogelbaum, M. A.; Bruce, J. N. Convection-enhanced drug delivery for glioblastoma: a review. *J. Neuro-Oncol.* **2021**, *151*, 415–427.
- (9) Mehta, A. M.; Sonabend, A. M.; Bruce, J. N. Convection-enhanced delivery. *Neurotherapeutics* **2017**, *14*, 358–371.
- (10) Bailly, C.; Vidal, A.; Bonnemaire, C.; Kraeber-Bodéré, F.; Chérel, M.; Pallardy, A.; Rousseau, C.; Garcion, E.; Lacoëuille, F.; Hindré, F.; et al. Potential for nuclear medicine therapy for glioblastoma treatment. *Front. Pharmacol.* **2019**, *10*, 772.
- (11) Li, Y.; Marcu, L. G.; Hull, A.; Bezak, E. Radioimmunotherapy of glioblastoma multiforme - current status and future prospects. *Crit. Rev. Oncol. Hematol.* **2021**, *163*, 103395.
- (12) Reardon, D. A.; Quinn, J. A.; Akabani, G.; Coleman, R. E.; Friedman, A. H.; Friedman, H. S.; Herndon, J. E., 2nd; McLendon, R. E.; Pegram, C. N.; Provenzale, J. M.; et al. Novel human IgG_{2b}/murine chimeric antitenascin monoclonal antibody construct radio-labeled with ¹³¹I and administered into the surgically created resection cavity of patients with malignant glioma: phase I trial results. *J. Nucl. Med.* **2006**, *47*, 912–918.
- (13) Zalutsky, M. R.; Reardon, D. A.; Akabani, G.; Coleman, R. E.; Friedman, A. H.; Friedman, H. S.; McLendon, R. E.; Wong, T. Z.; Bigner, D. D. Clinical experience with alpha-particle emitting ²¹¹At: treatment of recurrent brain tumor patients with ²¹¹At-labeled chimeric antitenascin monoclonal antibody 81C6. *J. Nucl. Med.* **2008**, *49*, 30–38.
- (14) Phillips, W. T.; Bao, A.; Brenner, A. J.; Goins, B. A. Image-guided interventional therapy for cancer with radiotherapeutic nanoparticles. *Adv. Drug Deliv. Rev.* **2014**, *76*, 39–59.
- (15) Phillips, W. T.; Goins, B.; Bao, A.; Vargas, D.; Gutierrez, J. E.; Trevino, A.; Miller, J. R.; Henry, J.; Zuniga, R.; Vecil, G.; et al. Rhenium-186 liposomes as convection-enhanced nanoparticle brachytherapy for treatment of glioblastoma. *Neuro Oncol.* **2012**, *14*, 416–425.
- (16) Kassiss, A. I. Therapeutic radionuclides: biophysical and radiobiologic principles. *Semin. Nucl. Med.* **2008**, *38*, 358–366.
- (17) Vanpouille-Box, C.; Lacoëuille, F.; Belloche, C.; Lepareur, N.; Lemaire, L.; LeJeune, J. J.; Benoit, J. P.; Menei, P.; Couturier, O. F.; Garcion, E.; et al. Tumor eradication in rat glioma and bypass of immunosuppressive barriers using internal radiation with ¹⁸⁸Re-lipid nanocapsules. *Biomaterials* **2011**, *32*, 6781–6790.
- (18) Huang, F. Y.; Lee, T. W.; Chang, C. H.; Chen, L. C.; Hsu, W. H.; Chang, C. W.; Lo, J. M. Evaluation of ¹⁸⁸Re-labeled PEGylated nanoliposome as a radionuclide therapeutic agent in an orthotopic glioma-bearing rat model. *Int. J. Nanomed.* **2015**, *10*, 463–473.
- (19) Shultz, M. D.; Wilson, J. D.; Fuller, C. E.; Zhang, J.; Dorn, H. C.; Fatouros, P. P. Metallofullerene-based nanoplatfor for brain

tumor brachytherapy and longitudinal imaging in a murine orthotopic xenograft model. *Radiology* **2011**, *261*, 136–143.

(20) Wilson, J. D.; Broaddus, W. C.; Dorn, H. C.; Fatouros, P. P.; Chalfant, C. E.; Shultz, M. D. Metallofullerene-nanoplatfrom-delivered interstitial brachytherapy improved survival in a murine model of glioblastoma multiforme. *Bioconjugate Chem.* **2012**, *23*, 1873–1880.

(21) Pijeira, M. S. O.; Viltres, H.; Kozempel, J.; Sakmár, M.; Vlk, M.; İlem-Özdemir, D.; Ekinci, M.; Srinivasan, S.; Rajabzadeh, A. R.; Ricci-Junior, E.; et al. Radiolabeled nanomaterials for biomedical applications: radiopharmacy in the era of nanotechnology. *EJNMMI Radiopharm. Chem.* **2022**, *7*, 8.

(22) Yook, S.; Cai, Z.; Lu, Y.; Winnik, M. A.; Pignol, J. P.; Reilly, R. M. Intratumorally injected ^{177}Lu -labeled gold nanoparticles: gold nanoseed brachytherapy with application for neoadjuvant treatment of locally advanced breast cancer. *J. Nucl. Med.* **2016**, *57*, 936–942.

(23) Wuithschick, M.; Birnbaum, A.; Witte, S.; Sztucki, M.; Vainio, U.; Pinna, N.; Rademann, K.; Emmerling, F.; Kraehnert, R.; Polte, J. Turkevich in new robes: key questions answered for the most common gold nanoparticle synthesis. *ACS Nano* **2015**, *9*, 7052–7071.

(24) Yook, S.; Lu, Y.; Jeong, J. J.; Cai, Z.; Tong, L.; Alwarda, R.; Pignol, J. P.; Winnik, M. A.; Reilly, R. M. Stability and biodistribution of thiol-functionalized and ^{177}Lu -labeled metal chelating polymers bound to gold nanoparticles. *Biomacromolecules* **2016**, *17*, 1292–1302.

(25) Yook, S.; Cai, Z.; Lu, Y.; Winnik, M. A.; Pignol, J. P.; Reilly, R. M. Radiation nanomedicine for EGFR-positive breast cancer: panitumumab-modified gold nanoparticles complexed to the beta-particle-emitter, ^{177}Lu . *Mol. Pharm.* **2015**, *12*, 3963–3972.

(26) Etame, A. B.; Diaz, R. J.; O'Reilly, M. A.; Smith, C. A.; Mainprize, T. G.; Hynynen, K.; Rutka, J. T. Enhanced delivery of gold nanoparticles with therapeutic potential into the brain using MRI-guided focused ultrasound. *Nanomedicine* **2012**, *8*, 1133–1142.

(27) Schulz, J. A.; Rodgers, L. T.; Kryscio, R. J.; Hartz, A. M. S.; Bauer, B. Characterization and comparison of human glioblastoma models. *BMC Cancer* **2022**, *22*, 844.

(28) Biedermann, K. A.; Sun, J. R.; Giaccia, A. J.; Tosto, L. M.; Brown, J. M. scid mutation in mice confers hypersensitivity to ionizing radiation and a deficiency in DNA double-strand break repair. *Proc. Natl. Acad. Sci. U.S.A.* **1991**, *88*, 1394–1397.

(29) Coluccia, D.; Figueiredo, C. A.; Wu, M. Y.; Riemenschneider, A. N.; Diaz, R.; Luck, A.; Smith, C.; Das, S.; Ackerley, C.; O'Reilly, M.; et al. Enhancing glioblastoma treatment using cisplatin-gold-nanoparticle conjugates and targeted delivery with magnetic resonance-guided focused ultrasound. *Nanomedicine* **2018**, *14*, 1137–1148.

(30) Stine, C. A.; Munson, J. M. Convection-enhanced delivery: connection to and impact of interstitial fluid flow. *Front. Oncol.* **2019**, *9*, 966.

(31) Loevinger, R.; Budinger, T. F.; Watson, E. *E.MIRD Primer for Absorbed Dose Calculations*, Revised Ed.; The Society of Nuclear Medicine Inc: New York, NY, 1991.

(32) Lam, K.; Chan, C.; Done, S. J.; Levine, M. N.; Reilly, R. M. Preclinical pharmacokinetics, biodistribution, radiation dosimetry and acute toxicity studies required for regulatory approval of a clinical trial application for a phase I/II clinical trial of ^{111}In -BzDTPA-pertuzumab. *Nucl. Med. Biol.* **2015**, *42*, 78–84.

(33) Bitar, A.; Lisbona, A.; Thedrez, P.; Maurel, C.; Forestier, D.; Barbet, J.; Bardies, M. A voxel-based mouse for internal dose calculations using Monte Carlo simulations (MCNP). *Phys. Med. Biol.* **2007**, *52*, 1013–1025.

(34) Lai, P.; Cai, Z.; Pignol, J. P.; Lechtman, E.; Mashouf, S.; Lu, Y.; Winnik, M. A.; Jaffray, D. A.; Reilly, R. M. Monte Carlo simulation of radiation transport and dose deposition from locally released gold nanoparticles labeled with ^{111}In , ^{177}Lu or ^{90}Y incorporated into tissue implantable depots. *Phys. Med. Biol.* **2017**, *62*, 8581–8599.

(35) Eckerman, K. F.; Endo, A. *MIRD Radionuclide Data and Decay Schemes*; Society of Nuclear Medicine, 2008.

(36) Zhou, Y.; Peng, Z.; Seven, E. S.; Leblanc, R. M. Crossing the blood-brain barrier with nanoparticles. *J. Controlled Release* **2018**, *270*, 290–303.

(37) Behroozi, Z.; Rahimi, B.; Kookli, K.; Safari, M. S.; Hamblin, M. R.; Razmgir, M.; Janzadeh, A.; Ramezani, F. Distribution of gold nanoparticles into the brain: a systematic review and meta-analysis. *Nanotoxicology* **2021**, *15*, 1059–1072.

(38) Lonser, R. R.; Sarntinoranont, M.; Morrison, P. F.; Oldfield, E. H. Convection-enhanced delivery to the central nervous system. *J. Neurosurg.* **2015**, *122*, 697–706.

(39) Cai, Z.; Chattopadhyay, N.; Yang, K.; Kwon, Y. L.; Yook, S.; Pignol, J. P.; Reilly, R. M. ^{111}In -labeled trastuzumab-modified gold nanoparticles are cytotoxic in vitro to HER2-positive breast cancer cells and arrest tumor growth in vivo in athymic mice after intratumoral injection. *Nucl. Med. Biol.* **2016**, *43*, 818–826.

(40) Cikankowitz, A.; Clavreul, A.; Tétaud, C.; Lemaire, L.; Rousseau, A.; Lepareur, N.; Dabli, D.; Bouchet, F.; Garcion, E.; Menei, P.; et al. Characterization of the distribution, retention, and efficacy of internal radiation of ^{188}Re -lipid nanocapsules in an immunocompromised human glioblastoma model. *J. Neuro-Oncol.* **2017**, *131*, 49–58.

(41) Bobyk, L.; Edouard, M.; Deman, P.; Vautrin, M.; Pernet-Gallay, K.; Delaroché, J.; Adam, J. F.; Estève, F.; Ravanat, J. L.; Elleaume, H. Photoactivation of gold nanoparticles for glioma treatment. *Nano-medicine* **2013**, *9*, 1089–1097.

(42) Barani, I. J.; Larson, D. A. Radiation therapy of glioblastoma. *Cancer Treat Res.* **2015**, *163*, 49–73.

(43) Lawrence, Y. R.; Li, X. A.; el Naqa, I.; Hahn, C. A.; Marks, L. B.; Merchant, T. E.; Dicker, A. P. Radiation dose-volume effects in the brain. *Int. J. Radiat. Oncol., Biol., Phys.* **2010**, *76*, S20–S27.

(44) Jost, S. C.; Hope, A.; Kiehl, E.; Perry, A.; Travers, S.; Garbow, J. R. A novel murine model for localized radiation necrosis and its characterization using advanced magnetic resonance imaging. *Int. J. Radiat. Oncol., Biol., Phys.* **2009**, *75*, 527–533.

(45) Lira-Diaz, E.; Gonzalez-Pedroza, M. G.; Vasquez, C.; Morales-Luckie, R. A.; Gonzalez-Perez, O. Gold nanoparticles produce transient reactive gliosis in the adult brain. *Neurosci. Res.* **2021**, *170*, 76–86.

(46) Jost, S. C.; Collins, L.; Travers, S.; Piwnica-Worms, D.; Garbow, J. R. Measuring brain tumor growth: combined bioluminescence imaging-magnetic resonance imaging strategy. *Mol. Imag.* **2009**, *8*, 245–253.